Biosensors and Bioelectronics 41 (2013) 498–504

Contents lists available at SciVerse ScienceDirect

Biosensors and Bioelectronics

journal homepage: www.elsevier.com/locate/bios

Graphene quantum dots as a new substrate for immobilization and direct electrochemistry of glucose oxidase: Application to sensitive glucose determination

Habib Razmi *, Rahim Mohammad-Rezaei

Electroanalytical Chemistry Research Laboratory, Faculty of Sciences, Azarbaijan Shahid Madani University, P.O. Box 53714-161, Tabriz, Iran

ARTICLE INFO

Article history:
Received 5 July 2012
Received in revised form
27 August 2012
Accepted 9 September 2012
Available online 28 September 2012

Keywords:
Glucose oxidase
Graphene quantum dots
Carbon ceramic electrode
Biosensor

ABSTRACT

Graphene quantum dots (GQD) were introduced as a novel and suitable substrate for enzyme immobilization. Glucose oxidase (GOx) was immobilized on GQD modified carbon ceramic electrode (CCE) and well-defined quasi-reversible redox peaks were observed. The UV–vis photoluminescence spectroscopy, transition electron microscopy, field emission scanning electron microscopy, electrochemical impedance spectroscopy, and cyclic voltammetry techniques were used for characterizing the electrochemical biosensor. The electron transfer coefficient (α) and the heterogeneous electron transfer rate constant (k_s) for redox reaction of GOx were found to be 0.48 and 1.12 s^{-1}, respectively. The developed biosensor responds efficiently to glucose presence over the concentration range 5–1270 μM with the detection limit 1.73 μM ($S/N=3$) and sensitivity 0.085 μA μM^{-1} cm^{-2}. The high value of surface coverage GOx–GQD|CCE (1.8×10^{-9} mol/cm^2) and the small value of Michaelis–Menten constant (0.76 mM) confirmed an excellent loading of the enzyme and a high affinity of biosensor to glucose. High performance of the biosensor is attributed to the large surface-to-volume ratio, excellent biocompatibility of GQD, porosity of GQD|CCE, and the abundance of hydrophilic edges as well as hydrophobic plane in GQD which enhances the enzyme absorption on the electrode surface.

1. Introduction

Since its discovery in 2004 (Novoselov et al., 2004), there has been a lot of interest toward graphene. Graphene is a two dimensional honeycomb network of sp^2 hybridized carbon atoms having unique electrical, optical and structural properties being vastly studied for applications in analytical, bioimaging, catalysis and photovoltaic devices (Zhu et al., 2010; Liu et al., 2012; Xiang et al., 2012). Due to the remarkable conductivity, high surface to volume ratio, and good biocompatibility, a lot of electrochemical sensors and biosensors have been introduced based on graphene materials (Chen et al., 2010; Ping et al., 2012; Qian et al., 2010). Graphene is a semi-metal or zero-gap semiconductor; however, its bandgap magnitude can be altered by size, shape, thickness, and fraction of the sp^2 domains (Kosynkin et al., 2009; Li et al., 2008).

Graphene sheets smaller than 100 nm are called graphene quantum dots (GQD) having various electronic and optoelectronic properties due to quantum confinement and edge effects, making it an excellent candidate for construction of nanoscaled optical and electronic devices (Shen et al., 2011; Mueller et al., 2010; Yan et al., 2010). Due to stable luminescence, good biocompatibility, suitable conductivity, and low toxicity, GQD are demonstrated to be efficient in both bioimaging and biosensing applications (Zhu et al., 2011; Shen et al., 2012).

In the field of electrochemical sensors and biosensors, there has been a little attention to GQD. Zhao et al. (2011) have reported the fabrication of a sensitive biosensor based on the interaction between single-stranded DNA and GQD.

Over the past decade there has been a lot of interest in the development of new reagentless biosensors using direct electron transfer of immobilized enzymes on conducting substrates (Deng et al., 2009; Zhang et al., 2011; Liu and Ju, 2003; Guascito et al., 2011). Graphene has the ability to promote electron transfer reactions and has been frequently used as an electrode material (Gan and Hu, 2011; Kuila et al., 2011). Thus, various redox proteins or enzymes have been coupled with graphene based materials to construct third generation electrochemical biosensors (Wu et al., 2010, Zeng et al., 2010).

In this research, to explore the enzyme absorption ability of GQD and its function in electron transfer promotion, glucose oxidase (GOx) was chosen as a model enzyme and the fabricated biosensor was studied in detail from the viewpoint of electrochemical behaviors and electrocatalytic properties.

* Corresponding author. Tel.: +98 4124322135; fax: +98 4124327541.
E-mail address: h.razmi@azaruniv.edu (H. Razmi).

0956-5663/$ - see front matter © 2012 Elsevier B.V. All rights reserved.
http://dx.doi.org/10.1016/j.bios.2012.09.009

At the first stage, GQD was simply coated on carbon ceramic electrode (CCE) surface (Tsionsky and Lev, 1995) by the drop-casting method. Then, the GQD modified CCE was activated and coated with GOx. The biosensor (GOx–GQD|CCE) was characterized by the UV–vis, photoluminescence spectroscopy, field emission scanning electron microscopy, electrochemical impedance spectroscopy, and cyclic voltammetry techniques thoroughly. Finally, GOx–GQD|CCE has been examined as a sensitive third-generation amperometric and voltammetric glucose biosensor in human serum analysis with satisfactory results.

2. Experimental

2.1. Chemicals and reagents

Glucose oxidase (from *Aspergillus niger*, E.C. 1.1.3.4) was obtained from Sigma Chemical (USA) and the stock solution was prepared in 0.05 M phosphate buffer solution (PBS) pH 7.4 and stored at 4 °C. D(+)-glucose, methyltrimethoxysilane, $K_3[Fe(CN)_6]$ and graphite fine powder were purchased from Merck. All other chemicals were of analytical grade and were used without further purification.

2.2. Apparatus

The electrochemical experiments were carried out using an AUTOLAB PGSTAT-100 (potentiostat/galvanostat) at room temperature. The utilized three-electrode system was composed of a saturated (KCl) calomel electrode (SCE) as the reference electrode, a platinum wire as the auxiliary electrode and the prepared electrode as the working electrode (surface area of 0.119 cm^2). A T80 UV–vis spectrophotometer (PG Instrument Ltd, England) and FP-6200 spectrofluorometer (JASCO Corporation, Tokyo, Japan) were used for recording the absorbance and Fluorescence spectra respectively. Electrochemical impedance spectroscopy (EIS) was performed in 0.1 M KNO_3 solution containing 5 mM $Fe(CN)_6^{3-}/Fe(CN)_6^{4-}$ (1:1) as a supporting electrolyte at its open circuit potential with a frequency range from 1.0×10^{-2} to 1.0×10^{5} Hz, using an alternating current voltage of 5 mV. The morphology of the electrodes was studied by field emission scanning electron microscopy (FESEM; Hitachi, model S-4160).

2.3. Synthesis of graphene quantum dots (GQD)

In this study, the hydrothermal method was used for synthesis of GQD (Pan et al., 2010). Firstly, graphene oxide was prepared by chemical oxidization of graphite powder according to the modified Hummers method (Xu et al., 2008). The as prepared graphene oxide was deoxidized in a tube furnace at 200–300 °C for 2 h and a heating rate of 5 °C min^{-1} in a nitrogen atmosphere. The obtained graphene sheets (0.05 g) were oxidized in concentrated H_2SO_4 (10 mL) and HNO_3 (30 mL) for 15–20 h under mild ultrasonication (500 W, 40 kHz). The oxidized graphene sheets were diluted and purified with microporous membrane and redispersed in deionized water. Then the suspension was heated at 200 °C for 10 h in an autoclave. The resulting black suspension was filtered with microporous membrane and a brown filter solution was obtained. To remove larger graphene nanoparticles, the colloidal solution was dialyzed in a dialysis bag (retained molecular weight: 3500 Da) overnight and GQD were obtained having stability for more than 3 months.

2.4. Preparation of GOx–GQD modified CCE

Due to some unique properties of carbon ceramic electrode (CCE) involving high porosity, renewable surface, good conductivity, and economy it was used as the biosensor substrate. CCE was prepared according to the procedure described by Tsionsky and Lev (1995). 0.3 mL MTMOS, 0.45 mL methanol, and 10 μL hydrochloric acid (11 M) were mixed for 3 min. Afterward, 0.3 g carbon powder was added and the resultant mixture was shaken for about 1 min. A piece of Teflon tube was filled with the sol–gel mixture, and was dried overnight under ambient conditions (ca. 25 °C). The electrode was polished with polishing paper and subsequently was rinsed with double distilled water.

15 μL of GQD solution was cast on the surface of CCE and dried overnight at room temperature to obtain a homogeneous GQD|CCE. Pretreatment is usually required to activate the surface of carbon electrodes (Pournaghi-Azar et al., 2006; Lin et al., 2006). To activate the surface of GQD|CCE, pre-treatment was performed potentiostatically at 1.7 V for 300 s. Finally 10 μL of GOx suspension (2 mg mL^{-1}) was cast onto the GQD|CCE surface using a syringe to prepare the GOx–GQD modified CCE (GOx–GQD|CCE). For slow evaporation of water and also for uniform film formation, a beaker was covered over the electrodes. Modified electrodes were stored at 4 °C when not in use.

3. Results and discussion

3.1. Characteristics of GOx–GQD modified CCE

UV–vis absorption and photoluminescence spectroscopy are two techniques in the assay of the as prepared GQD. Fig. 1A shows the absorbance (curve a) and photoluminescence (curve b) of GQD. A broad UV–vis absorption with a weak shoulder at 320 nm and also photoluminescence spectrum peak (under excitation at 320 nm) at 413 nm are characteristics of GQD according to previous reports (Pan et al., 2010; Shen et al., 2011).

Fig. 1B shows the TEM image of GQD showing monodispersity and particle size of the GQD sheets. Also, the morphologies of GQD|CCE and GOx–GQD|CCE were studied by FESEM. As shown in Fig. 1C and D, piecemeal and wrinkled GQD sheets on the surface of the CCE were constructed, and the multi-pore and scaly network surface of CCE changed to a uniform and three dimensional layered GQD film (the magnifications are 1500 for Fig. 1B and 20,000 for Fig. 1D). The porous and layered structure of GQD|CCE is beneficial to the mass transfer of electroactive species and the stabilization of the dispersed biomaterials. As can be seen, the enzyme successfully distributed on GQD|CCE and a compact and uniform film has been formed (Fig. 1E).

3.2. Electrochemical impedance spectroscopy studies

EIS is a helpful technique providing detailed information on the impedance changes of the electrode interface. In a typical impedance spectrum, a semicircle part at higher frequencies and a straight line at lower frequencies correspond to the electron transfer-limit process and diffusion-limit process, respectively. The charge transfer resistance (Rct) can be estimated by the semicircle diameter of the impedance spectra at high frequency. Herein, EIS was employed to investigate the Rct of $Fe(CN)_6^{3-/4-}$ as a redox probe at the surface of CCE, GQD|CCE and GOx–GQD|CCE. Fig. 2A shows the Nyquist plots of the electrodes in 5 mM $Fe(CN)_6^{3-/4-}$ containing 0.1 M KNO_3 as the supporting electrolyte. The impedance spectrum of the CCE (Fig. 2A, curve a) exhibited an almost straight line at all frequencies corresponding to the diffusion process. The low Rct on the bare CCE indicated the fast electron transfer rate between CCE and $Fe(CN)_6^{3-/4-}$. The diameter of the semicircle for GQD|CCE (Fig. 2A, curve b) was larger than that of bare CCE, indicating that the GQD on the surface of CCE decreased the electron transfer rate between the redox probe of

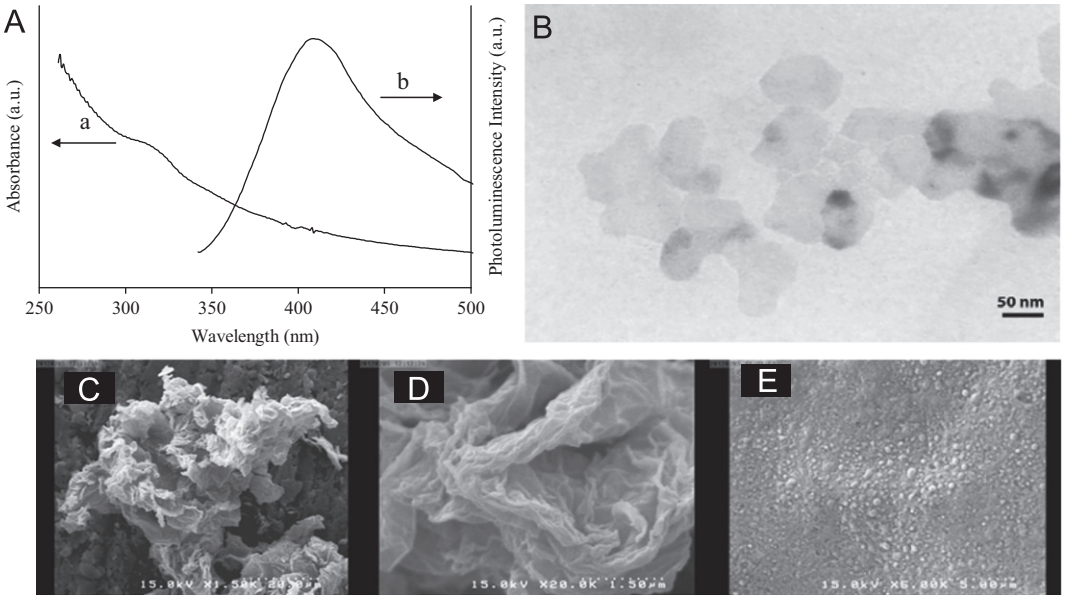

Fig. 1. (A) UV–vis spectra (curve a) and photoluminescence (curve b) of GQD, (B) TEM image of GQD, (C, D) FESEM of GQD modified CCE with magnitude of 1500 and 20,000 respectively and (E) FESEM of GOx–GQD|CCE.

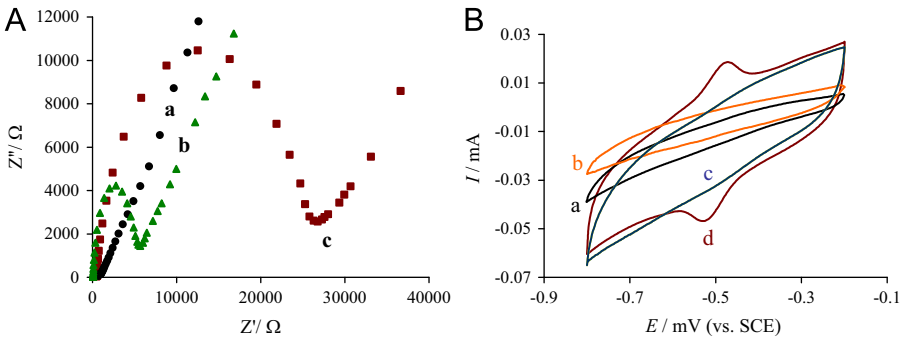

Fig. 2. (A) EIS of CCE (curve a), GDQ|CCE (curve b) and GOx–GQD|CCE (curve c) and (B) CVs of CCE (curve a), GOx|CCE (curve b), GQD|CCE (curve c) and GOx–GQD|CCE (curve d) in PBS 0.1 M, pH 7 and scan rate of 100 mV s^{-1}.

$Fe(CN)_6^{3-/4-}$ and the electrode surface. Plenty of polar and negatively charged oxygen functional groups such as –COOH prevent $Fe(CN)_6^{3-/4-}$ from penetrating the electrode/solution interference. Also, in comparison with graphene which is a metal-like conductor, GQD has semiconductor properties and its conductivity is lower than that of graphene (Rao et al., 2009; Son et al., 2006; Wei and Liu, 2010).

GQD has shown size tuneable properties such as increase of energy gap (E_g) with decrease in its size. Thus increase of semicircle in impedance spectra can be proportional to GQD energy gap. Therefore, E_g of GQD can be estimated from the Rct. Thus we can offer an initial equation

$$E_g \propto K(\mathrm{Rct}) \quad (1)$$

where K is the proportionality coefficient and its magnitude depends on the GQD size and degree of semiconductivity of GQD. Future studies are in progress for developing the relation of Rct and GQD sheets size.

When GOx was assembled on the surface of GQD|CCE, Rct increased dramatically (Fig. 2A, curve c) due to the higher hindrance at the surface of modified electrode confirming successful immobilization of GOx on the surface of GQD|CCE. Although GQD is not an excellent conductive material, high surface area of GQD, hydrophilic edges, good biocompatibility, and favorable orientation of GOx, and also hydrophobic interactions between GQD plane and GOx lead to a multivalent interaction between the GQD and enzyme resulting in strong absorption of enzyme on the surface of GQD. Considering low toxicity and eco-friendly properties of GQD and its function in increasing the electron transfer of enzyme, GQD can be introduced as a new substrate for efficient enzyme immobilization.

3.3. Direct electrochemistry of GOx–GQD|CCE

Direct electrochemistry of GOx immobilized on GQD|CCE was investigated using cyclic voltammetry in N_2-saturated 0.1 M PBS, pH 7.4 at the scan rate of 100 mV s^{-1}. As shown in Fig. 2B, no redox peak was observed at the bare CCE (curve a), GOx|CCE (curve b) and GQD|CCE (curve c). However, a pair of well-defined and quasi-reversible redox peaks was observed at the GOx–GQD|CCE (curve d) with the formal peak potential −0.509 V and peak-to-peak separation (ΔE_p) 42 mV. These redox peaks are characteristic of reversible electron transfer process of redox active center (flavin adenine dinucleotide, FAD) in the GOx (Wang et al., 2006; Shangguan et al., 2008) proving a fast electron transfer process.

Considering EIS and CV studies, significant enhancement of GOx absorption on the GQD surface and also, direct electron transfer of GOx can be concluded.

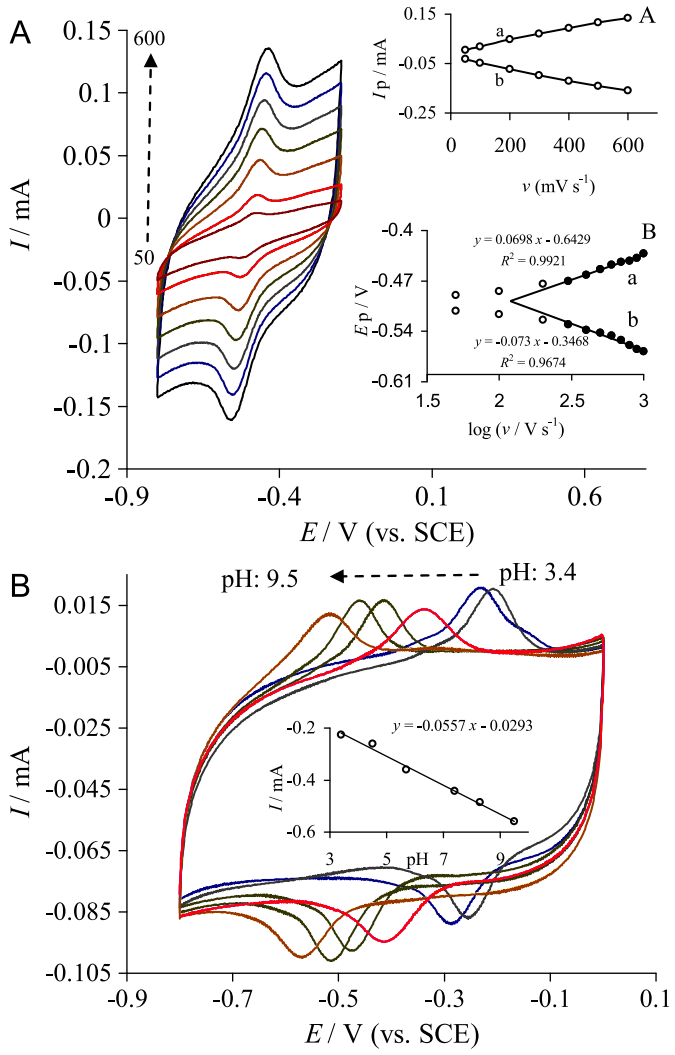

Fig. 3. (A) CVs of GOx–GQD|CCE at different scan rates (from inner to outer: 50–600 mV s^{-1}), insets (A and B) are plots of anodic and cathodic peak currents vs. scan rate and peak potentials vs. log scan rates respectively. (B) CVs of GOx–GQD|CCE in different pH solutions (3.4–9.5), scan rate 300 mV s^{-1}. Inset is the plot of formal potential vs. pH values.

Fig. 3A shows the CVs of the GOx–GQD|CCE in N_2-saturated PBS at various scan rates. With increasing scan rate, both redox peak currents and peak-to-peak separation increase. The peak currents increase with scan rate in the range from 50 to 600 mV s^{-1} (Fig. 3A, inset A) indicating that the electrochemical behavior of GOx has the typical property of a surface electrochemical process. The cathodic and anodic peak currents were of similar magnitude, with a ratio of about unity.

The anodic and cathodic peak potentials were linearly dependent on the logarithm of the scan rates (v) with slopes of $2.3RT/(1-a)nF$ and $-2.3RT/anF$, respectively (Fig. 3A, inset B). Thus, the charge-transfer coefficient (a) was calculated to be 0.48. The heterogeneous electron transfer rate constant (k_s) was further estimated according to the following equation:

$$\log k_s = \alpha\ \log(1-\alpha) + (1-\alpha)\log\alpha - \log\frac{RT}{nFv} - \frac{\alpha(1-\alpha)nF\,\Delta E_p}{2.3RT} \quad (2)$$

where α is the charge transfer coefficient; n is the number of electron transfer; R, T and F symbols have their conventional meanings; and ΔE_p is the peak to peak potential separation. Taking the scan rate 400 mV s^{-1}, k_s was calculated to be 1.12 s^{-1}.

For thin layer voltammetry, integration of CV peaks gives the total amount of charge (Q) passed through the electrode for the reduction or oxidation of electroactive enzymes. The surface coverage (Γ) of electroactive GOx in GOx–GQD|CCE can be estimated to be 1.8×10^{-9} mol cm^{-2} from integration of the anodic and cathodic peaks of the CVs according to $\Gamma = Q/nFA$, where Q is the charge involved in the reaction, n is the number of electron transferred, F the Faraday constant, and A is the electrode area (0.119 cm^2). This value is much larger than that of monolayer coverage of GOx on the bare electrode surface which was calculated to be 2.86×10^{-12} mol cm^{-2} (Zhang et al., 2007), indicating that a multilayer and three-dimensional coverage of GOx has been formed on GQD. High surface area and good biocompatibility of GQD has increased the absorption of GOx and also surface area of GOx–GQD|CCE.

3.4. Influence of solution pH

It is well known that the direct electrochemistry of GOx is a two-electron coupled with two-proton reaction, which undergoes a redox reaction as follows:

$$\mathrm{GOx\,(FAD)} + 2e^- + 2H^+ \rightleftharpoons \mathrm{GOx\,(FADH_2)} \quad (3)$$

Therefore, the pH value of the solution has influence on the electrochemical behavior of GOx at the GOx–GQD|CCE. Fig. 3B shows the cyclic voltammograms of the GOx–GQD|CCE in the solutions with different pH values (3.4–9.5) at a scan rate of 300 mV s^{-1}. As can be seen, a pair of stable and well-defined reversible redox peaks is obtained on GOx–GQD|CCE at different solution pHs. The peak potentials shift to negative direction (inset of Fig. 3B) when solution pH increases from 3.4 to 9.5. The slope is −55.7 mV/pH, which is close to the theoretical value of −58.5 mV/pH (Huang et al., 2005), proving participation of two protons ($2\,H^+$) and two electrons ($2e^-$) in the electrode reaction.

3.5. Response characteristics of the biosensor to glucose

It is well known that GOx usually exhibits good electrocatalytic activity toward oxygen and H_2O_2 when immobilized on electrode surface (Kang et al., 2009). Herein, to investigate the bio-electrocatalytic activity of the GOx–GQD|CCE toward the reduction of oxygen, cyclic voltammetry experiments were performed. Fig. 4A shows the CVs of GOx–GQD|CCE in N_2 saturated (curve a), O_2 saturated (curve b) and O_2-saturated PBS containing 2 mM glucose (curve c). As shown in Fig. 4A (curve a), a pair of symmetrical redox peaks in N_2-saturated solution was observed, indicating that GOx undergoes a reversible electrochemical reaction (Eq. 3). The shape of redox peaks for the direct electron transfer of GOx changes dramatically in the presence of oxygen (Fig. 4A, curve b) as the reduction peak current increases whereas the oxidation peak current decreases. The electrocatalytic process of GOx–GQD|CCE is expressed as follows (Liu and Ju, 2003):

$$\mathrm{GOx(FADH_2)} + O_2 \rightarrow \mathrm{GOx(FAD)} + H_2O_2 \quad (4)$$

The changes in anodic and cathodic peaks confirm that GOx in the GOx–GQD|CCE catalyzed the reduction of oxygen with the EC_{cat} mechanism (Eqs. (3) and (4)).

Upon addition of glucose (2 mM), the reduction peak current decreases due to the decrease of oxygen on the electrode surface caused by enzyme-catalyzed reaction between the oxidized form of GOx, GOx (FAD), and glucose according to the following equation (Fig. 4A, curve b):

$$\mathrm{Glucose} + \mathrm{GOx(FAD)} \rightarrow \mathrm{gluconolactone} + \mathrm{GOx(FADH_2)} \quad (5)$$

The current decrease is proportional to the addition of glucose concentration (Fig. 4B), suggesting the employment of this

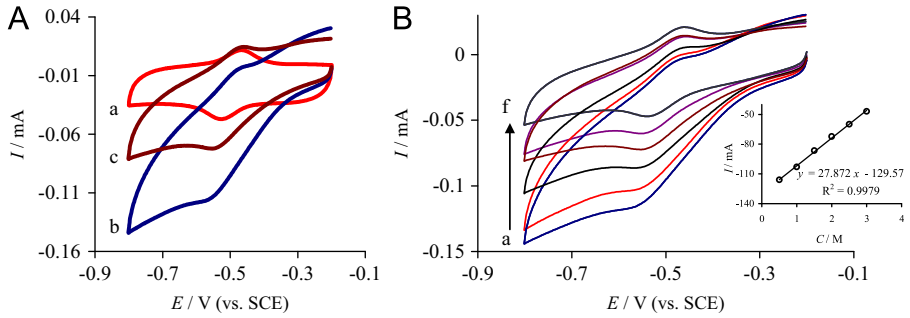

Fig. 4. (A) CVs of GOx–GQD|CCE in (a) N_2-saturated, O_2-saturated PBS 0.1 M pH 7.4 in the (b) absence and (c) presence of 2 mM glucose at 100 mV s^{-1}. (B) CVs of the GOx–GQD|CCE in air-saturated PBS at scan rate of 100 mV s^{-1} with the addition of 0.5 mM (a), 1 mM (b), 1.5 mM (c), 2 mM (d), 2.5 mM (e) and 3 mM glucose.

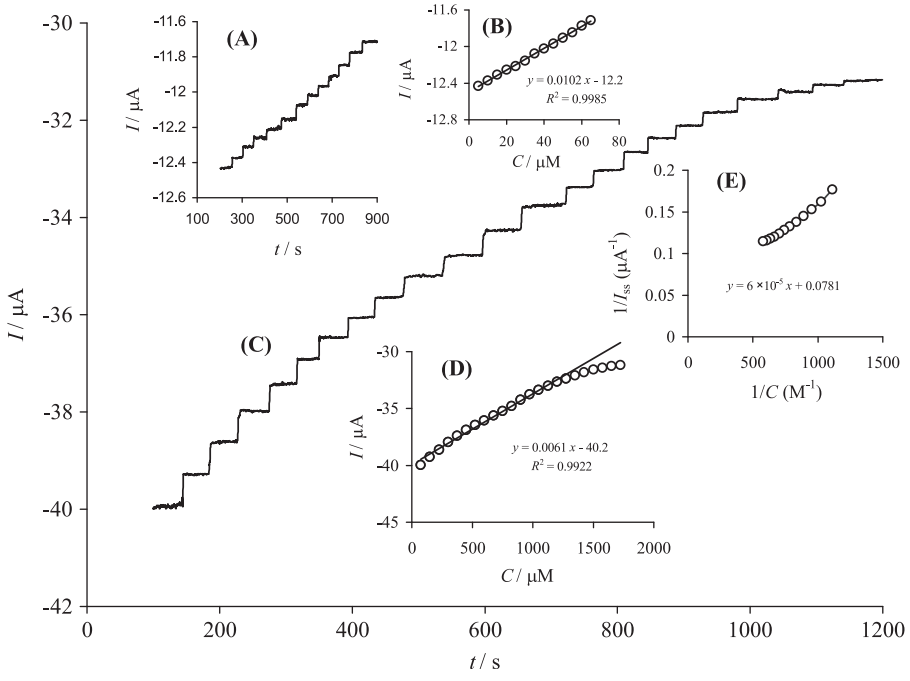

Fig. 5. Amperometric response of GOx–GQD|CCE to glucose, conditions: −0.42 V constant potential, PBS 0.1 M, pH 7.4; (A) successive addition of 5 µM and (C) 75 µM; (B) and (D) show the plot of chronoamperometric current vs. glucose concentration which was obtained from (A) and (C) amperograms. and (E) Lineweaver–Burk plot for K_m value determination.

response for determination of the glucose concentration. The inset of Fig. 4B represents the relation between the reduction peak current of GOx–GQD|CCE and the concentration of glucose. As shown, the peak currents decreased linearly with the glucose concentration in the range 0.5–3 mM.

To further illustrate the relationship between the electrocatalytic reduction current and the concentration of glucose, the chronoamperometry technique was performed at a conditional potential −0.42 V in PBS 0.1 M, pH 7.4. The steady-state current obtained on the GOx–GQD|CCE decreased during the successive addition of glucose concentration (Fig. 5A and C). The electrocatalytic response was very fast as the biosensor achieved more than 97% of the maximum response after 3 s when glucose was added into the electrolyte solution. The plot of current response vs. glucose concentration was linear over the wide concentration ranges 5–60 µM (Fig. 5B) and 75 µM–1.27 mM (Fig. 5D). The calibration plot over the concentration range 5–60 µM exhibited a sensitivity 0.085 µA μM^{-1} cm^{-2}, correlation coefficient 0.9985 and detection limit 1.73 µM ($S/N = 3$). Analytical figures of merit for determination of glucose were compared with some reported glucose biosensors and the results are summarized in Table 1. The sensitivity, linear range and detection limit of developed biosensor were improved and are comparable with recent reports.

When the concentration of glucose was higher than 1.27 mM, the electrode response deviated from linearity and levelled off, showing the characteristics of the Michaelis–Menten kinetic mechanism. The Michaelis–Menten constant is an important parameter for revealing enzyme–substrate reaction kinetics which can be obtained from the Lineweaver–Burk equation as follows (Li et al., 1996):

$$\frac{1}{I_{ss}} = \frac{1}{I_{\max}} + \frac{K_m}{I_{\max}}\frac{1}{C} \quad (6)$$

where C is the concentration of glucose in solution, I_{ss} is the catalytic current (background current deducted) at the steady state when glucose concentration is at C, and I_{max} is the maximum catalytic current. K_m can be obtained by the analysis of the slope and the intercept of the plot of the reciprocals of the steady-state current vs. glucose concentration (Fig. 5E). The amount of this constant (K_m) was calculated to be 0.76 mM which was compared with those of other glucose biosensors in Table 1. The lower magnitude of K_m confirms the retention of GOx native structure in

Table 1
Analytical figures of merit of some glucose biosensors.

Modified electrode	Linear range (μM)	Sensitivity	LOD (μM)	K_m (mM)	Ref.
ZnO/GOx/MWCNTs	6.67–1290	0.01003 μA μM^{-1} cm^{-2}	2.22	2.4	Hu et al., 2011
Nafion/GOx/Ag Pdop@CNT/GCE	50–1100	0.0031 μA μM^{-1}	17	5.46	Wang et al., 2011
GOx–graphene-chitosan	80–12000	0.03793 μA μM^{-1} m^{-2}	20	–	Kang et al., 2009
CS–GOD–CdS/ACNTs–Pt nano	400–21,200	0.045 μA μM^{-1}	46.8	11.86	Jing et al., 2008
SPE/sol–gel–PVA–GOx	100–4550	0.00347 μA μM^{-1} cm^{-2}	9.8	–	Zuo et al., 2008
Graphene–Pt/GCE	150–10000	0.00192 μA μM^{-1}	80	2.5	Sheng et al., 2009
Cu-NPs/ZnO/GC	1–1530	0.16 μA mM^{-1}	0.2	–	Kumar et al., 2010
Ag-NPs/PVA/Pt	10–15000	0.143 and 0.094 μA cm^{-2} μM^{-1}	0.4	–	Guascito et al., 2011
GOx–GQD|CCE	5–1270	0.085 μA μM^{-1} cm^{-2}	1.73	0.76	This work

GOx–GQD|CCE, resulting in higher affinity and activity of the GOx toward the glucose in an enzymatic reaction.

3.6. Reproducibility and stability of the GOx–GQD|CCE

The reproducibility and stability of GOx–GQD|CCE as well as its response reproducibility to glucose were investigated by cyclic voltammetry in PBS 0.1 M, pH 7.4. When the electrode potential was swept cyclically in the range 0 to −0.8 V at a scan rate of 100 mV s^{-1} for 200 cycles, the peak currents remained almost 95% of the initial response and peak potential remained unchanged proving the excellent stability of the fabricated modified electrode. Also integration of the cathodic peak currents of the five independently prepared modified electrodes has shown that the relative standard deviation (RSD%) value is 5%, confirming appropriate reproducibility of the modified electrode.

Furthermore, three electrodes showed acceptable reproducibility in response to 2 mM glucose (RSD 5%). In addition, after being stored for 2 weeks, the response to 2 mM glucose decreased by only 7%, indicating the suitable stability of GOx–GQD|CCE. Good reproducibility and stability of the biosensor can be attributed to the porous nature of CCE, high surface to volume ratio of GQD and strong interaction between enzyme and GQD. The above results prove the suitability of our simple immobilization procedure which retained the electrocatalytic activity of GOx and prevented it from leaking out of the electrode surface proving its capability in marketing.

3.7. Interference study and determination of glucose in human plasma sample

Under the optimal conditions for determination of glucose, interferences of some substances that exist in biological liquids were investigated. The interference tests were carried out by the amperometric technique in the presence of 100 μM glucose and the same concentrations of uric acid, ascorbic acid, dopamine and some amino acids such as L-tryptophan, L-tyrosine, and L-cysteine. There was no obvious change in the glucose signal when these substances were added to the electrolyte solution.

In order to investigate the possible application of the developed biosensor in clinical analysis, GOx–GQD|CCE was used for determination of blood sugar concentration in human plasma samples using the standard addition method. Based on this study, the glucose concentration in blood was found to be 4.7 mM. Also the accuracy of the biosensor was evaluated by recovery test. Recoveries from 95.1% to 106.5% ($n=6$) were obtained when different amounts of glucose were spiked before any pretreatment to the samples. The result demonstrated good accuracy for the determination of glucose in real samples, ascertaining the practical application of the proposed glucose biosensor in clinical analysis.

4. Conclusions

A new, simple and low cost glucose biosensor based on GOx–GQD|CCE was developed. Electrochemical techniques as well as morphology studies of the biosensor confirmed the outstanding function of GQD in electrochemical biosensors. High level stability, sensitivity and accuracy of the biosensor in determination of glucose which arose from high surface to volume ratio, good biocompatibility and excellent ability of GQD for enzyme immobilization are its important advantages for application in practical and routine analyses.

Acknowledgment

The authors gratefully acknowledge the Research Council of Azarbaijan Shahid Madani University for financial support. Our thanks also go to M. Akbari-Moghanjoughi, from Department of Physics, Azarbaijan Shahid Madani University, for helpful comments.

References

Chen, D., Tang, L., Li, J., 2010. Chemical Society Reviews 39, 3157–3180.
Deng, S., Jian, G., Lei, J., Hu, Z., Ju, H., 2009. Biosensors and Bioelectronics 25, 373–377.
Gan, T., Hu, S., 2011. Microchimica Acta 175, 1–19.
Guascito, M.R., Chirizzi, D., Picca, R.A., Malitesta, C., Mazzotta, E., 2011. Analyst 136, 164–173.
Huang, Y., Zhang, W., Xiao, H., Li, G., 2005. Biosensors and Bioelectronics 21 (5), 817–821.
Hu, F., Chen, S., Wang, C., Yuan, R., Chai, Y., Xiang, Y., Wang, C., 2011. Journal of Molecular Catalysis B: Enzymatic 72, 298–304.
Kang, X., Wang, J., Wu, H., Aksay, I.A., Liu, J., Lin, Y., 2009. Biosensors and Bioelectronics 25 (4), 901–905.
Kosynkin, D.V., Higginbotham, A.L., Sinitskii, A., Lomeda, J.R., Dimiev, A., Price, B.K., Tour, J.M., 2009. Nature 458, 872–876.
Kuila, T., Bose, S., Khanra, P., Mishra, A.K., Kim, N.H., Lee, J.H., 2011. Biosensors and Bioelectronics 26, 4637–4648.
Kumar, S., Cheng, H., Chen, S., Wang, S., 2010. Materials Science and Engineering C 30, 86–91.
Li, J., Tan, S.N., Ge, H., 1996. Analytica Chimica Acta 335, 137–145.
Li, X.L., Wang, X.R., Zhang, L., Lee, S.W., Dai, H.J., 2008. Science 319, 1229–1232.
Lin, X.Q., He, J.B., Zha, Z.G., 2006. Sensors and Actuators B 119 (2), 608–614.
Liu, S., Ju, H., 2003. Biosensors and Bioelectronics 19, 177–183.
Liu, Y., Dong, X., Chen, P., 2012. Chemical Society Reviews 41, 2283–2307.
Mueller, M.L., Yan, X., McGuire, J.A., Li, L.S., 2010. Nano Letters 10 (7), 2679–2682.
Novoselov, K.S., Geim, A.K., Morozov, S.V., Jiang, D., Zhang, Y., Dubonos, S.V., Grigorieva, I.V., Firsov, A.A., 2004. Science 306 (5696), 666–669.
Ping, J., Wu, J., Wang, Y., Ying, Y., 2012. Biosensors and Bioelectronics 34, 70–76.
Pan, D., Zhang, J., Li, Z., Wu, M., 2010. Advanced Materials 22, 734–738.
Pournaghi-Azar, M.H., Hejazi, M.S., Alipour, E., 2006. Analytica Chimica Acta 570 (2), 144–150.
Qian, J., Zhang, C., Cao, X., Liu, S., 2010. Analytical Chemistry 82, 6422–6429.
Rao, C.N.R., Sood, A.K., Subrahmanyam, K.S., Govindaraj, A., 2009. Angewandte Chemie International Edition 48 (42), 7752–7777.
Shangguan, X., Zhang, H., Zheng, J., 2008. Electrochemistry Communications 10 (8), 1140–1143.
Shen, J., Zhu, Y., Chen, C., Yang, X., Li, C., 2011. Chemical Communications 47, 2580–2582.
Shen, J., Zhu, Y., Yang, X., Li, C., 2012. Chemical Communications 48, 3686–3699.
Sheng, Q., Luo, K., Li, L., Zheng, J., 2009. Bioelectrochemistry 74, 246–253.

Son, Y.W., Cohen, M.L., Louie, S.G., 2006. Physical Review Letters 97, 216803–216806.
Tsionsky, M., Lev, O., 1995. Analytical Chemistry 67, 2409–2414.
Wang, Y.D., Joshi, P.P., Hobbs, K.L., Johson, B.B., Schmidtke, D.W., 2006. Langmuir 22 (23), 9776–9783.
Wang, Y., Liu, L., Li, M., Xu, S., Gao, F., 2011. Biosensors and Bioelectronics 30, 107–111.
Wei, D., Liu, Y., 2010. Advanced Materials 22 (30), 3225–3241.
Wu, P., Shao, Q., Hu, Y., Jin, J., Yin, Y., Zhang, H., Cai, C., 2010. Electrochimica Acta 55, 8606–8614.
Xiang, Q., Yu, J., Jaroniec, M., 2012. Chemical Society Reviews 41, 782–796.
Xu, Y., Bai, H., Lu, G., Li, C., Shi, G., 2008. Journal of the American Chemical Society 130 (18), 5856–5857.
Yan, X., Cui, X., Li, L.S., 2010. Journal of the American Chemical Society 132, 5944–5945.
Zhang, J., Feng, M., Tachikawa, H., 2007. Biosensors and Bioelectronics 22, 3036–3041.
Zhang, H., Meng, Z., Wang, Q., Zheng, J., 2011. Sensors and Actuators B 158, 23–27.
Zeng, G., Xing, Y., Gao, J., Wang, Z., Zhang, X., 2010. Langmuir 26 (18), 15022–15026.
Zhao, J., Chen, G., Zhu, L., Li, G., 2011. Electrochemistry Communications 13, 31–33.
Zhu, Y., Murali, S., W-Cai, W., Li, X., Suk, J.W., Potts, J.R., Ruoff, R.S., 2010. Advanced Materials 22, 3906–3924.
Zhu, S., Zhang, J., Qiao, C., Tang, S., Li, Y., Yuan, W., Li, B., Tian, L., Liu, F., Hu, R., Gao, H., Wei, H., Zhang, H., Sun, H., Yang, B., 2011. Chemical Communications 47, 6858–6860.
Zuo, S., Teng, Y., Yuan, H., Lan, M., 2008. Sensors and Actuators B 133, 555–560.